The Canadian Mineralogist
Vol. 45, pp. 239-248 (2007)

THE CRYSTAL STRUCTURE OF Si-DEFICIENT, OH-SUBSTITUTED, BORON-BEARING VESUVIANITE FROM THE WILUY RIVER, SAKHA-YAKUTIA, RUSSIA

EVGENY V. GALUSKIN[§] AND IRINA O. GALUSKINA

Faculty of Earth Sciences, Department of Geochemistry, Mineralogy and Petrography, University of Silesia, Będzińska 60, 41–200 Sosnowiec, Poland

KATARZYNA STADNICKA

Faculty of Chemistry, Jagiellonian University, Ingardena 3, Cracow, 30–060, Poland

THOMAS ARMBRUSTER

Laboratory for Chemical and Mineralogical Crystallography, University of Bern, Freiestr. 3, CH–3012 Bern, Switzerland

MARCIN KOZANECKI

Technical University, Department of Molecular Physics, Żeromskiego 116, 90–924 Łódź, Poland

ABSTRACT

The crystal structure of a Si-deficient vesuvianite, space group *P4/nnc*, *a* 15.678(1), *c* 11.828(1) Å, from the Wiluy River, Sakha–Yakutia, Russia, has been refined from single-crystal X-ray data to $R = 0.037$. Electron-microprobe analyses indicate that this vesuvianite has only *ca*. 16 Si *pfu* in contrast to regular vesuvianite with 18 Si *pfu*. Site-occupancy refinement yielded substantial vacancies at orthosilicate sites *Z*(1): 25% vacancies, *Z*(2): 16% vacancies. Vacancies at the tetrahedral site are associated with increased *Z*(1)–O and *Z*(2)–O distances, 1.687 and 1.660 Å, respectively. Vacancies and increased *Z*(1)–O and *Z*(2)–O bond lengths are consistent with hydrogarnet-type defects, where SiO_4 is replaced by H_4O_4 tetrahedra. The single crystal investigated shows the highest hydrogarnet-type substitution analyzed by structure refinement of vesuvianite. No vacancies were found involving the disilicate groups. Along the **c** axis, the increased size of *Z*(1) tetrahedra is balanced by a compression of the adjacent *X*(3) Ca-bearing dodecahedra. This structural flexibility is the reason why the length of the **c** axis remains largely independent of the hydrogarnet-type substitution. A corresponding structural flexibility does not exist along the **a** axis, leading to a systematic increase of *a* with increasing proportion of vacancies at the Si site. Polarized Raman spectra in the OH-stretching region are interpreted to indicate that hydrogarnet-type defects in vesuvianite lead to a more isotropic polarization of the absorption bands at about 3650 cm^{-1}.

Keywords: Si-deficient vesuvianite, composition, crystal structure, Raman spectra, hydrogarnet-type defects, Yakutia, Russia.

SOMMAIRE

Nous avons affiné la structure cristalline d'un monocristal de vésuvianite déficitaire en Si, groupe spatial *P4/nnc*, *a* 15.678(1), *c* 11.828(1) Å, provenant d'un site sur la rivière Wiluy, Sakha–Yakutia, en Russie, avec données en diffraction X jusqu'à un résidu *R* de 0.037. Les analyses obtenues avec une microsonde électronique indiquent que cet échantillon ne possède qu'environ 16 atomes de Si par unité formulaire, au lieu de 18 dans la vésuvianite régulière. Un affinement de l'occupation des sites révèle la présence de lacunes importantes au sites orthosilicate *Z*(1): 25% de lacunes, *Z*(2): 16% de lacunes. Les lacunes à ces sites tétraédriques sont associées à une augmentation des distances *Z*(1)–O et *Z*(2)–O, 1.687 et 1.660 Å, respectivement. La présence de lacunes et les distances *Z*(1)–O et *Z*(2)–O accrues seraient dues à la présence de défauts de type hydrogrenat, dans lesquels SiO_4 est remplacé par des tétraèdres H_4O_4. Le monocristal étudié témoigne du taux de substitution du type hydrogrenat le plus élevé parmi les cristaux de vésuvianite dont la structure a été affinée. Aucune lacune n'a été trouvée dans les groupes disilicatés. Le long de l'axe **c**, la plus grande dimension des tétraèdres *Z*(1) est contre-balancée par la compression des dodécaèdres à Ca [*X*(3)] adjacents. Cette flexibilité structurale explique pourquoi la longueur de la maille dans la direction de l'axe **c** demeure relativement insensible au taux de substitution de type hydrogrenat. Une flexibilité structurale correspondante n'existe pas le

§ *E-mail address*: galuskin@us.edu.pl

long de l'axe **a**, et explique l'allongement systématique de *a* à mesure qu'augmente la proportion de lacunes au site Si. D'après les spectres de Raman polarisés dans la région de l'étirement des groupes OH, les défauts de type hydrogrenat sont à l'origine de la polarisation plus isotrope des bandes d'absorption à environ 3650 cm^{-1}.

(Traduit par la Rédaction)

Mots-clés: vésuvianite déficitaire en Si, composition, structure cristalline, spectre de Raman, défauts de type hydrogrenat, Yakoutie, Russie.

Introduction

Silicon deficient, OH-substituted, boron-bearing vesuvianite of simplified composition $Ca_{19}(Al,Mg,Fe,Mn)_{13}B_{<2.5}[(SiO_4)_{10-x}(OH)_{4x}](Si_2O_7)_4(OH,O,F,Cl)_{10}$, where $x < 3$, was recently discovered along the banks of the Wiluy River, Sakha–Yakutia, Russia (Galuskin *et al*. 2003a). The same deposit is known as the type locality for grossular, wiluite, and "achtarandite", an unusual tetrahedral pseudomorph of hibschite after a wadalite-like mineral (Lyakhovich 1954, Groat *et al*. 1998, Galuskin *et al*. 1995, Galuskina *et al*. 1998).

In this paper, we present the structural peculiarities of the Si-deficient vesuvianite, established on the basis of single-crystal X-ray structure refinements and on single-crystal Raman investigations. Our work complements our description of the morphology, crystal chemistry, and genetic conditions of Si-deficient vesuvianite (Galuskin *et al*. 2003a).

Background Information

A general crystal-chemical formula for the vesuvianite group of minerals may be given as $X_{18}X'Y'Y_{12}T_{0-5}(ZO_4)_{10}(Z_2O_7)_4O_{1-2}W_9$ or $Ca_{19}(Al,Mg,Fe,Mn,Ti\ldots)_{13}(B,Al,\square\ldots)_5(SiO_4)_{10}(Si_2O_7)_4O_{1-2}$ $(OH,O,F,Cl)_9$ (Warren & Modell 1931, Coda *et al*. 1970, Yoshiasa & Matsumoto 1986, Allen & Burnham 1992, Fitzgerald *et al*. 1992, Groat *et al*. 1992, Ohkawa 1994, Armbruster & Gnos 2000a, b). The *X'* and *Y'* positions are placed along the fourfold axes in the structural channels. The group of vesuvianite minerals consists of vesuvianite, wiluite, fluorvesuvianite, and manganvesuvianite. In wiluite, more than 2.5 B *pfu* occupy the *T* sites (Groat *et al*. 1998), in fluorvesuvianite, F exceeds 4.5 *apfu* at the *W* site (Britvin *et al*. 2003), and in manganvesuvianite, Mn^{3+} exceeds 0.5 *apfu* at the *Y'* site (Armbruster *et al*. 2002).

Silicon-deficient vesuvianite differs from ordinary vesuvianite by a significant hydrogarnet-type substitution $SiO_4^{4-} \rightarrow H_4O_4^{4-}$ restricted to the isolated *Z*-tetrahedra (Armbruster & Gnos 2000b, Galuskin *et al*. 2003a). Silicon-deficient vesuvianite at the Wiluy locality occurs in rodingite-like rocks formed at the expense of high-temperature melilite-bearing skarns. It is found (1) inside tetrahedral pseudomorphs of hibschite after a wadalite-like mineral, (2) as a part of a polymineralic pseudomorph after boron-enriched gehlenite, and (3) as thin zones on wiluite crystals (Galuskin & Galuskina 2002, Galuskin *et al*. 2003a, Galuskin 2005).

The Material Available for Study and Methods of Investigation

Light-cream-colored Si-deficient vesuvianite occurs in association with hibschite and chlorite. Owing to non-stationary conditions of growth, these crystals of vesuvianite are usually developed as subindividuals and have been described as vesuvianite with split forms (Galuskin *et al*. 2003a). Such samples do not allow selection of structurally homogeneous single crystals. Crystals of Si-deficient vesuvianite were successfully extracted for our structural investigation from a sample representing an oriented intergrowth of the tetrahedral pseudomorph of hibschite ("achtarandite", ~0.5 cm across) with a large crystal of yellow-green grossular {211} (~1.8 cm) [epitaxy of wadalite-like protophase of "achtarandite" on grossular (Galuskin *et al*. 1995, Galuskina *et al*. 1998)]. The surface of grossular is covered by an epitactic layer of hibschite up to 40 μm thick. Silicon-deficient vesuvianite with split forms is commonly found inside domains of "achtarandite" (Fig. 1a). Rather well-developed crystals of Si-deficient vesuvianite (Fig. 1b) were discovered on the epitactic layer of hibschite. However, the homogeneous outer appearance of these crystals contrasts with their internal heterogeneity. They consist of irregular growth-sectors formed of very spongy domains (Fig. 1c).

An investigation of crystal morphology and the selection of crystals of Si-deficient vesuvianite for single-crystal investigation of the structure were done with a scanning electron microscope ESEM FEI/Philips XL30 in the low-vacuum condition at 0.2–0.4 Torr, with a back-scattered-electron (BSE) detector used with on uncoated samples. Quantitative analyses of vesuvianite (Table 1) were carried out with a CAMECA SX100 electron microprobe. Analytical details have been described by Galuskin *et al*. (2003a, b).

Single-crystal X-ray-diffraction data were collected for a prismatic crystal of Si-deficient vesuvianite (0.18 × 0.18 × 0.11 mm) using a Bruker SMART CCD single-crystal X-ray diffractometer with graphite-monochromated Mo*K*α X-radiation. Diffraction data were collected with an exposure time of 10 s per frame. Longer exposure-times, up to 300 s per frame, were also

attempted in order to resolve additional low-intensity reflections characteristic of the space groups *P*4*nc* and *P*4/*n*. However, such datasets suffered from the low quality of the crystal, leading to split or diffuse reflections, the intensity of which could not be satisfactory integrated. Furthermore, the high background-noise of such datasets did not yield information on possible weak reflections indicating deviations from space group *P*4/*nnc*.

The cell dimensions were refined from angular settings of 37 reflections with $10 < 2\theta < 32.6°$, yielding tetragonal symmetry. Diffraction data collected up to $2\theta = 55.94°$, yielding 1717 unique reflections, of which 1175 had $F > 4\sigma(F)$, were used for structure solution and refinement. Experimental details are shown in Table 2. The structure was successfully solved in space group *P*4/*nnc* and subsequently refined using the SHELXL–97 program (Sheldrick 1997). Cation occupancy is based on electron density and interatomic distances. Coordinates and site occupancies of the atoms are given in Table 3. Anisotropic displacement-parameters are given in Table 4, and selected interatomic distances are summarized in Table 5.

Raman spectra were recorded using a Jobin–Yvon Raman microprobe T–64000 with a 514.5 nm Ar ion laser. The power at the exit 50× or 100× objective varied from 200 to 500 mW. The polarized spectra were recorded in 180° geometry, in the range 50–4000 cm^{-1} of Raman shift, with a spectral resolution of 3.5 cm^{-1}. Collection time (60–300 s) and accumulation of 3–10 scans were chosen depending on the properties of the crystal investigated (*i.e.*, character of fluorescence, stability).

The table of structure factors and a digital version of the Raman spectra are available from are available from the Depository of Unpublished Data on the MAC web site [document vesuvianite CM45_239].

TABLE 1. CHEMICAL COMPOSITION OF VESUVIANITE FROM A RODINGITE-LIKE ROCK, YAKUTIA

	1	2	3	4	5	6	7
SiO_2 wt%	32.15	32.17	33.21	33.73	33.70	36.31	33.53
SO_3	0.09	0.13	0.04	0.12	n.d.	0.01	0.07
TiO_2	0.03	n.d.	0.12	0.04	n.d.	0.17	0.06
B_2O_3	1.44	1.01	0.83	1.22	1.15	1.48	0.98
Al_2O_3	16.73	17.10	16.03	16.22	16.23	14.24	16.18
MgO	4.58	3.22	4.48	4.61	4.31	4.66	4.52
CaO	38.07	37.02	37.01	37.14	37.15	35.35	37.11
MnO	0.47	0.47	0.39	0.37	0.28	0.34	0.40
Fe_2O_3 [x]	1.46	3.36	1.77	1.58	1.73	4.24	1.60
H_2O [xx]	5.80	4.50	4.92	4.35	4.64	1.00	4.69
F	0.26	0.89	0.27	0.22	0.25	0.22	0.24
Cl	0.19	0.35	0.12	0.12	0.06	n.d.	0.12
–O = F + Cl	0.15	0.45	0.14	0.12	0.12	0.09	0.12
Total	101.12	99.77	99.05	99.60	99.38	97.93*	99.38
O_{calc}	44.27	42.00					
O_{exp}	43.57	42.14					
Ca *apfu*	19	19	19	19	19	19	19
Ti	0.01		0.04	0.02		0.06	0.02
Al	9.11	9.30	8.96	8.98	9.13	7.70	9.02
Mg	3.18	2.30	3.20	3.28	3.06	3.48	3.22
Mn^{2+}	0.19	0.19	0.16	0.15	0.11	0.14	0.16
Fe^{3+}	0.51	1.21	0.64	0.57	0.62	1.62	0.58
Y site	13	13	13	13	12.92	13	13
B	1.16	0.83	0.69	1.01	0.95	1.28	0.81
Al	0.07	0.36	0.10	0.14		0.72	0.09
T site	1.23	1.19	0.79	1.15	0.95	2.00	0.90
Si	14.97	15.41	15.92	16.11	16.09	18.21	16.02
S^{6+}	0.03	0.05	0.01	0.05		0.01	0.03
Z site	15	15.46	15.93	16.15	16.09	18.22	16.05
OH	18.02	14.38	15.73	13.86	14.77	3.35	14.95
F	0.38	1.35	0.40	0.34	0.38	0.35	0.36
Cl	0.15	0.29	0.09	0.09	0.05		0.09

Columns: 1–2: split crystals of Si-deficient vesuvianite as shown in Figure 1a; 3–6: more regular crystal of Si-deficient vesuvianite with rim of vesuvianite, point of analyses shown in Figure 1b; 7: mean result of eight analyses of Si-deficient vesuvianite analogous to the crystal used for the structural investigation. [x]: Total Fe as Fe_2O_3. [xx]: OH calculated to satisfy balance of valences. * The total includes 0.03 Cr_2O_3; n.d.: not detected.

Results and Discussion

In our description of the morphology and composition of Si-deficient boron-bearing vesuvianite from the Wiluy River (Galuskin *et al*. 2003a), we noted that this material is characterized by a lower Si content, as low as 15 a*pfu* Si, and increased unit-cell parameters (powder-diffraction data): *a* 15.688(3), *c* 11.860(3) Å. The single crystal of Si-deficient vesuvianite reported in this study has a lower proportion of hydrogarnet-type defects (~16 Si *pfu*) and also smaller unit-cell dimensions: *a* 15.678(1), *c* 11.828(1) (Tables 1, 2). Good agreement was obtained between a crystal-chemical formula calculated on the basis of electron-microprobe analyses of a similar crystal (Table 1, anal. 7) and the formula derived from the structure refinement (Table 3). This is rather surprising considering the spongy nature of the crystal, composed of irregular growth-sectors.

TABLE 2. EXPERIMENTAL DATA AND INFORMATION ON THE REFINEMENT OF Si-DEFICIENT VESUVIANITE

Diffractometer	Bruker SMART CCD
X-ray radiation	fine-focus sealed tube Mo*Kα* (0.71073 Å)
Monochromator	graphite
Temperature	293(2) K
Space group	*P*4/*nnc*, no. 126
a, *c* (Å), *V* (Å^3)	15.678(1), 11.828(1), 2907.3(3)
Crystal size (mm)	0.18 × 0.11
Index range	$-13 \le h \le 20$, $-19 \le k \le 20$, $-14 \le l \le 15$
Upper 2θ limit	55.94
Reflections collected	15057
Unique reflections	1717
Reflections > 4σ(*F*)	1175
Number of parameters	168
Absorption corrections	empirical: Ψ scan
R_{int}, R_σ	0.0777, 0.0547
GooF	1.036
*R*1, $F_o > 4\sigma(F)$	0.0370
*R*1, all data	0.0639
w*R*2 (on F^2)	0.0928

TABLE 3. POSITIONAL PARAMETERS OF ATOMS, SITE OCCUPANCY AND U_{eq} VALUES FOR Si-DEFICIENT VESUVIANITE

atom	occupancy		*x/a*	*y/b*	*z/c*	U_{eq}
	site	*apfu*				
X(1)		2Ca	0.75	0.25	0.75	0.01807(38)
X(2)		8Ca	0.68891(5)	0.04439(5)	0.87814(7)	0.01699(22)
X(3)		8Ca	0.40049(6)	0.18009(6)	0.60724(8)	0.02965(26)
X'(4)	0.5	Ca	0.75	-0.25	0.85351(28)	0.01690(72)
Y'(1)		0.527(10)Fe + 0.473(10)Al	0.75	-0.25	0.95483(35)	0.0317(14)
Y(2)		4Al	0.5	0	0.5	0.01617(36)
Y(3)		8Al	0.61234(7)	0.38005(7)	0.87360(10)	0.01545(28)
Z(1)	0.748(8)	1.495(17)Si + 2.02H^{x}	0.75	0.25	1	0.01093(92)
Z(2)	0.842(4)	6.738(32)Si + 5.05H^{x}	0.54229(8)	0.18060(8)	0.87209(10)	0.01283(43)
Z(3)		8	0.65065(7)	-0.08408(8)	0.63561(9)	0.01705(27)
O(1)			0.72007(17)	0.32942(16)	0.91234(23)	0.02004(64)
O(2)			0.61819(17)	0.15945(17)	0.77901(22)	0.01998(65)
O(3)			0.54820(17)	0.27829(17)	0.92458(23)	0.02002(64)
O(4)			0.56310(17)	0.10551(17)	0.97153(21)	0.01973(64)
O(5)			0.67020(16)	0.01257(17)	0.67890(22)	0.01902(64)
O(6)			0.72558(18)	-0.12034(18)	0.55705(22)	0.02455(71)
O(7)			0.44543(20)	0.17227(20)	0.82196(28)	0.03679(85)
O(8)			0.59180(16)	-0.06063(16)	0.93132(22)	0.01796(64)
O(9)			0.64567(17)	-0.14567(17)	0.75	0.02038(88)
O(10)	1.103(21)	1.82(2)O$^{\blacklozenge}$ + 0.18Cl	0.25	0.25	0.64874(70)	0.0672(34)
O(11)	1	8O$^{\clubsuit}$	0.43760(18)	-0.00323(19)	0.86201(23)	0.02173(65)
T(1)	0.067(18)	0.27B	0.4436(69)	0.0564(69)	0.75	0.05*
T(2)	0.216(8)	0.22B	0.25	0.25	0.75	0.05*
H(1)	0.7	5.6H	0.4702(41)	0.0064(50)	0.8098(50)	0.05*

H^{x} = 4(*Z* – Si), O$^{\blacklozenge}$ = O + F + OH, O$^{\clubsuit}$ = O + F, Al = Al + Mg, Fe = Fe + Mn. The refined formula is: $Ca_{19}[(Al,Mg)_{12.47}(Fe,Mn)_{0.53}]_{\Sigma 13}B_{0.49}[(SiO_4)_{8.23}(H_4O_4)_{1.77}]_{\Sigma 10}(Si_2O_7)_4[OH_{5.6}(O,F)_{2.4}]_{\Sigma 8}[(O,OH,F)_{1.82}Cl_{0.18}]_{\Sigma 2}$. Note: U_{eq} values with an asterisk were fixed in the refinement.

TABLE 4. ANISOTROPIC DISPLACEMENT PARAMETERS FOR Si-DEFICIENT VESUVIANITE FROM WILUY RIVER

atom	U_{11}	U_{22}	U_{33}	U_{23}	U_{13}	U_{12}
X(1)	0.02298(91)	0.01571(85)	0.01553(85)	0	0	0
X(2)	0.01541(42)	0.01942(44)	0.01615(43)	0.00096(33)	0.00182(35)	-0.00147(33)
X(3)	0.02418(52)	0.02343(50)	0.04135(62)	-0.00296(44)	0.01190(43)	-0.00186(38)
X'(4)	0.0144(11)	0.0144(11)	0.0219(20)	0	0	0
Y'(1)	0.0216(15)	0.0216(15)	0.0519(30)	0	0	0
Y(2)	0.01591(83)	0.01484(82)	0.01776(86)	0.00030(72)	-0.00177(72)	-0.00044(75)
Y(3)	0.01528(61)	0.01629(63)	0.01478(61)	-0.00107(48)	0.00204(50)	0.00059(48)
Z(1)	0.0108(11)	0.0108(11)	0.0111(16)	0	0	0
Z(2)	0.01434(72)	0.01176(71)	0.01238(72)	0.00121(54)	0.00153(51)	0.00063(50)
Z(3)	0.01509(58)	0.01972(61)	0.01632(57)	0.00177(47)	-0.00068(45)	-0.00160(49)
O(1)	0.0190(15)	0.0208(15)	0.0204(15)	-0.0045(12)	0.0017(13)	-0.0009(12)
O(2)	0.0195(15)	0.0192(16)	0.0212(16)	0.0016(12)	0.0003(12)	-0.0007(12)
O(3)	0.0223(16)	0.0212(15)	0.0166(15)	0.0019(13)	0.0002(12)	0.0023(12)
O(4)	0.0200(16)	0.0191(15)	0.0200(16)	-0.0020(12)	0.0026(12)	-0.0016(12)
O(5)	0.0178(15)	0.0233(15)	0.0159(15)	0.0004(13)	-0.0003(12)	-0.0044(13)
O(6)	0.0210(16)	0.0319(17)	0.0208(16)	0.0061(13)	0.0029(12)	0.0019(13)
O(7)	0.0305(19)	0.0432(22)	0.0366(20)	0.0032(17)	0.0001(16)	-0.0053(15)
O(8)	0.0180(15)	0.0180(15)	0.0179(15)	-0.0006(11)	0.0023(12)	-0.0015(12)
O(9)	0.0220(13)	0.0220(13)	0.0172(21)	0.0007(13)	0.0007(13)	-0.0007(19)
O(10)	0.0508(35)	0.0508(35)	0.1001(73)	0	0	0
O(11)	0.0221(16)	0.0226(16)	0.0205(16)	0.0031(13)	0.0008(12)	0.0009(14)

In addition, the crystal investigated is covered by a thin (2–3 μm) layer of ordinary vesuvianite (Fig. 1c, Table 1). This thin layer probably did not influence the results of the structure refinement.

The structure of the crystal of Si-deficient vesuvianite investigated was refined in space group *P*4/*nnc*. At first glance, this symmetry seems to be inconsistent with its low-temperature genesis and high Al content, a characteristic of vesuvianite from rodingites. A comparison of polarized Raman spectra of low-temperature *P*4/*n* vesuvianite from rodingites and high-temperature *P*4/*nnc* wiluite with the spectra of Si-deficient vesuvianite indicates that the spectrum of the latter is closer to that of disordered high-temperature wiluite (Fig. 2; Paluszkiewicz & Żabiński 2004). The complex chemical composition with elevated boron, F and Cl content, combined with the $H_4O_4 \rightarrow SiO_4$ substitution, may have prevented string order during crystal growth. For a discussion on intra-string disorder in low-temperature vesuvianite, see Galuskin *et al*. (2003b).

In general, earlier refinements of the structure of vesuvianite gave *Z*(1)–O distances in the range 1.63–1.64 Å and a mean *Z*(2)–O distance of 1.64–1.65 Å (Groat *et al*. 1992, Ohkawa 1994, Lager *et al*. 1999, Armbruster *et al*. 2000a, c, Galuskin *et al*. 2003b). In Si-deficient vesuvianite from the Wiluy deposit, *Z*(1)–O is 1.687 Å, and *Z*(2)–O (mean) is 1.660 Å. These values are significantly larger than the above reference values. Structure refinements of Mn-bearing vesuvianite with hydrogarnet defects were previously reported for samples from South Africa (Armbruster & Gnos 2000b). The South African vesuvianite from the Kalahari manganese fields displays up to 14% vacancies at *Z*(1) and up to 5% at *Z*(2), respectively. Corresponding *Z*(1)–O and *Z*(2)–O distances are 1.665 and 1.648 Å, respectively. It is known that an increase of the observed Si–O distance in hydrogarnet is proportional to the

TABLE 5. SELECTED INTERATOMIC DISTANCES IN Si-DEFICIENT VESUVIANITE FROM WILUY RIVER

atom	-atom	[Å]	atom	-atom	[Å]
X(1)	- O(1) × 4	2.336(3)	*Y*(1)	- O(6) × 4	2.073(3)
	- O(2) × 4	2.530(3)		- O(10)	2.294(9)
mean		2.433	mean		2.117
X(2)	- O(1)	2.473(3)	*Y*(2)	- O(4) × 2	1.957(3)
	- O(2)	2.420(3)		- O(8) × 2	1.907(3)
	- O(3)	2.390(3)		- O(11) × 2	1.904(3)
	- O(4)	2.455(3)	mean		1.922
	- O(5)	2.363(3)			
	- O(5)	2.427(3)	*Y*(3)	- O(1)	1.922(3)
	- O(6)	3.009(3)		- O(2)	1.911(3)
	- O(8)	2.329(3)		- O(3)	1.980(3)
mean		2.483		- O(4)	2.040(3)
				- O(5)	2.011(3)
X(3)	- O(3)	2.435(3)		- O(11)	1.939(3)
	- O(6)	2.464(3)	mean		1.967
	- O(6)	2.926(3)			
	- O(7)	2.424(3)	*Z*(1)	- O(1) × 4	1.687(3)
	- O(7)	2.560(3)			
	- O(7)	2.639(3)	*Z*(2)	- O(7)	1.636(3)
	- O(8)	2.572(3)		- O(2)	1.655(3)
	- O(10)	2.647(2)		- O(3)	1.655(3)
	- O(11)	2.476(3)		- O(4)	1.696(3)
mean		2.572	mean		1.660
X(4)	- O(6) × 4	2.323(3)	*Z*(3)	- O5	1.629(3)
	- O(9) × 4	2.617(4)		- O6	1.602(3)
mean		2.470		- O8	1.623(3)
				- O9	1.664(2)
T(1)	- O(11) × 2	1.62(6)	mean		1.629
	- O(7) × 2	2.01(6)			
mean		1.815			
T(2)	- O(10) × 2	1.198(8)	O(10)	- O(10)	2.396(4)

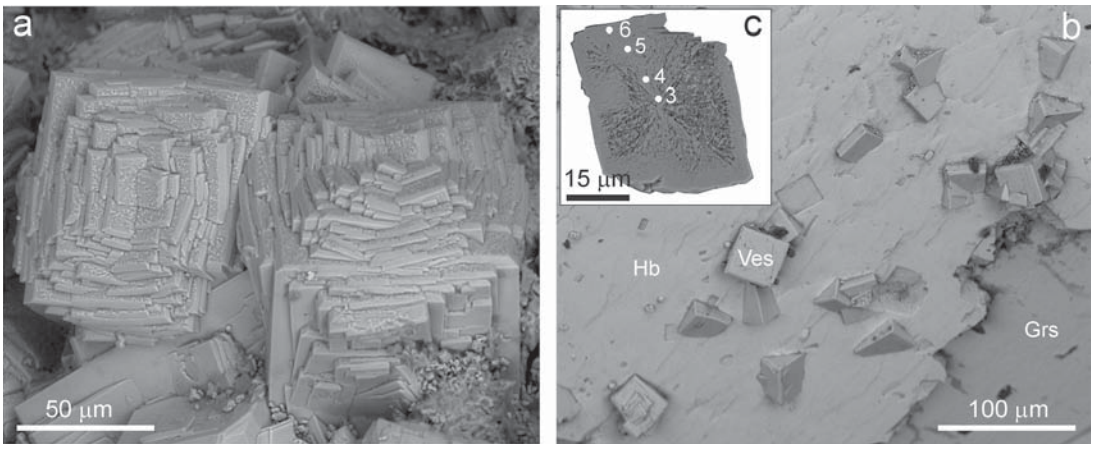

FIG. 1. a. Crystals of Si-deficient vesuvianite with splitting of (001) and (100) faces from "achtarandite" pseudomorph. b. Rather regular crystals of Si-deficient vesuvianite grown on a late zone of hibschite, epitactic on grossular. c. Cross section of a crystal shown in b: irregular growth sectors formed by strongly spongy domains. Locations of microprobe point-analyses are shown by numbered dots. Hb: hibschite, Grs: grossular, Ves: Si-deficient vesuvianite.

concentration of $H_4O_4 \rightarrow SiO_4$ (hydrogarnet) defects (Lager *et al*. 1989). In an anhydrous garnet, the Si–O distance is 1.63–1.64 Å. In Si-free katoite, the corresponding distance from the center of the vacant tetrahedron to the surrounding atoms of oxygen is 1.96–1.98 Å (Lager *et al*. 1989, Armbruster & Gnos 2000b). In the Si-deficient vesuvianite from the Wiluy deposit, the increased Si–O distances for the orthosilicate groups at *Z*(1) and *Z*(2) hence suggest a significant level of hydrogarnet-type substitution. Site-occupancy refinements of *Z*(1) (occupancy 75%) and *Z*(2) (occupancy 84%) are consistent with the increased Si–O distances (Table 5).

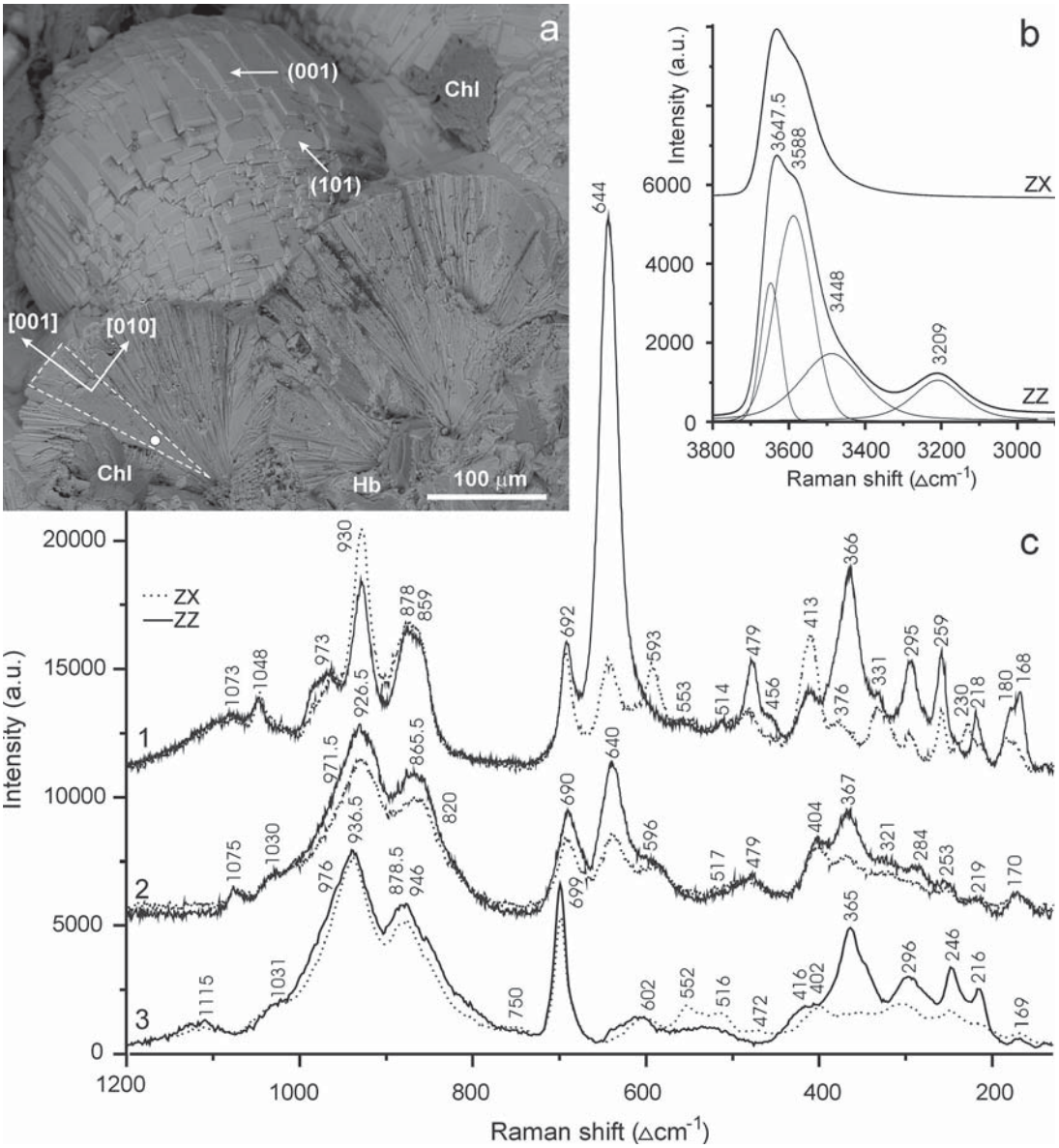

FIG. 2. a. Spherulites of pinacoidal type of Si-deficient vesuvianite. White point shows the spot of microRaman measurement on a natural (100) cleavage plane of a central crystal within the spherulite. Chl: chlorite. b. Polarized Raman spectrum of Si-deficient vesuvianite in the OH region. c. Raman spectrum of Si-deficient vesuvianite (2) in the fundamental Si–O region in comparison with ordered *P*4/*n* low-temperature vesuvianite from Kazakhstan rodingite (1) and with disordered *P*/4*nnc* high-temperature wiluite from the Wiluy deposit (3).

If the increased *Z*–O distances were caused by Al-for-Si substitution, the electron density on the *Z* sites would not be significantly reduced. Correspondingly, tetrahedrally coordinated boron at *Z* sites would decrease the electron density but would not increase *Z*–O distances. For this reason, identification of hydrogarnet-like defects in vesuvianite is rather straightforward.

The average Si–O distance for the disilicate group at *Z*(3) is 1.629 Å. Furthermore, *Z*(3) displays no vacancies, which is consistent with full occupancy by Si. The Si concentration determined by site-occupancy refinement of all *Z* sites (16.23 Si *pfu*) corresponds to the amount of silicon measured with the electron microprobe (Tables 1, 3). Electron-microprobe analyses with measured concentrations of oxygen indicate that hydrogen must be considered to compensate for Si vacancies (Table 1). The crystal investigated shows the greatest extent of hydrogarnet-type substitution hitherto demonstrated for vesuvianite by crystal-structure refinement. The preference for Si vacancies at *Z*(1) confirms previous findings (Armbruster & Gnos 2000b).

Increase of the size of the *Z*(1) tetrahedron (*Z*–O = 1.69 Å) in Si-deficient vesuvianite is compensated by compression of the eight-coordinated *X*(1) site (Ca dodecahedron) along the **c** axis. For fluorine-rich vesuvianite (Galuskin *et al*. 2003b), the height of the *Z*(1) tetrahedron along the **c** axis is 2.02 Å, and the corresponding height of the *X*(1) dodecahedron is 3.87 Å, whereas for Si-deficient vesuvianite, the height of the *Z*(1) tetrahedron along **c** is 2.075 Å and it is 3.84 Å for the *X*(1) dodecahedron (Fig. 3). Thus, the linear arrangement *Z*(1)–*X*(1)–*Z*(1)–*X*(1)–*Z*(1)… compensates for variable Si on *Z*(1) along the **c** axis (Fig. 3a). Moreover, the *X*(1)–*O*(1) bond lengths do not vary significantly among vesuvianite samples with *Z*(1) fully occupied and *Z*(1) partially vacant. The flexibility along **c** is accomplished by minor variations in the bond angles (Fig. 3). Thus, the unit-cell dimension *c*, in the range 11.83–11.86 Å in Si-deficient vesuvianite, is only insignificantly increased in comparison with the value in the range 11.80–11.84 Å (Fitzgerald *et al*. 1986, Groat *et al*. 1992, Pavese *et al*. 1998, Armbruster & Gnos 2000a, b, Galuskin *et al*. 2003a) for regular vesuvianite with 18 a*pfu* Si. A *c* repeat-distance of 12 Å as derived from powder-diffraction data (Henmi *et al*. 1994) for vesuvianite showing hydrogarnet-type substitution from alteration products of gehlenite is probably erroneous and due to misinterpreted admixtures of hydrogrossular in the sample.

In contrast, the vesuvianite structure does not exhibit such elasticity in directions perpendicular to the **c** axis (Tribaudino & Prencipe 2001). This causes a significant increase in length of the a axis, up to 15.68–15.69 Å for Si-deficient vesuvianite compared to vesuvianite with 18 Si *pfu* and *a* in the range 15.50–15.57 Å (Fitzgerald *et al*. 1986, Groat *et al*. 1992, Pavese *et al*. 1998, Armbruster & Gnos 2000a, c).

The mean *Y'*(1)–O distance (2.117 Å) for the square pyramidal site is relatively large in Si-deficient vesuvianite from the Wiluy River. This may be evidence in favor of the incorporation of Mg together with Fe. The mean *Y*(2)–O distance of 1.922 Å indicates that this position is filled by Al, whereas the *Y*(3)–O distance (1.967 Å) suggests significant Mg (*ca*. 3 *apfu* according to EMPA data in Table 1) in addition to Al.

The separation between adjacent *O*(10) sites in the channels of Si-deficient vesuvianite is anomalously short ~2.40 Å, but the displacement parameters of this site show a high degree of disorder along the fourfold axis ($U_{33} > U_{11}$; Tables 4, 5). A site-occupancy refinement for *O*(10) as well as results of electron-microprobe analyses suggest the presence of significant Cl at this site. This is also confirmed by increased *X*(3)–*X*(3) distances. The *X*(3) sites form a square centered by *O*(10) with edges of 3.68 Å. This increased edge-length is characteristic of Cl-bearing vesuvianite (Fig. 3, Okhawa 1994, Galuskin *et al*. 2003b, 2005). For *P*4/*nnc* vesuvianite with a high Cl content, >0.4–0.5 *apfu*, the *O*(10) site becomes split into two subsites *O*(10A) (occupied by O) and *O*(10B) (occupied by Cl + F). However, in the present study, the Cl concentration was not sufficiently high to resolve a splitting of *O*(10) (Table 3, Okhawa 1994).

An additional argument that the observed short *O*(10)–*O*(10) distance is an average comes from Raman spectroscopy. Raman investigations of Si-deficient vesuvianite show for polarized spectra in the OH region a weak broad line at 3209 cm^{-1} corresponding to the group *O*(10)–*H*(2)...*O*(10). The observed wavenumber and polarization indicate a hydrogen bond donor–acceptor distance $R_{O(10)–O(10)}$ of ~2.7 Å characteristic of disordered high-temperature vesuvianite (Groat *et al*. 1995, Paluszkiewicz & Żabiński 1995, 1999, Libowitzky 1999).

Another source of intra-channel disorder is the low occupancy (22%) of the interstitial *T*(2) site by boron (Fig. 3). In wiluite and samples of boron-rich vesuvianite with almost complete occupancy of *T*(2) by boron, one *O*(10) site is replaced by two *O*(12) sites, shifted from the four-fold axis, leading to triangular coordination of *T*(2) with B–O distances of approximately 1.35 Å (Ohkawa 1994, Groat *et al*. 1994, 1996, Bellatreccia *et al*. 2005a). In the present refinement of structure of the Si-deficient vesuvianite with a low B content at *T*(2) (0.22 B *pfu*), the low occupancy at *T*(2) did not allow us to resolve the true coordination of the B atom. Instead, the poorly defined electron-density of the coordinating *O*(12) sites contributes to the observed disorder and "smearing" of *O*(10).

The tetrahedral coordination of *T*(1) also is irregular, as it is made up of two *O*(11) sites 1.61 Å and two *O*(7) sites 2.01 Å from *T*(1). The low (*ca*. 7%) occupancy of boron at *T*(1) does not allow us to resolve the true coordination of the boron. For high occupancy by boron at *T*(1), *O*(7) splits into two subsites *O*(7A) and *O*(7B),

in which *O*(7B) contributes to the boron coordination [B–*O*(7B) = 1.64 Å] and *O*(7A) is associated with empty *T*(1) sites (Groat *et al*. 1996). The low occupancy of *T*(1) is the reason that only *O*(7A) is observed.

The same tetrahedron, *T*(1), also contains a network of hydrogen bonds. The *H*(1) sites are found 0.82 Å from *O*(11) and are connected by bifurcated hydrogen bonds to opposite *O*(7) and *O*(11) sites (Fig. 4). The *O*(7) site also takes part in the coordination of the *Z*(2) site (Fig. 4), for which 15% vacancies (85% Si) were determined. Charge balance for the vacant Z(2) sites is obtained by $4H^{+}$ instead of Si^{4+}, with formation of the so-called hydrogarnet defects. The exact position of protons in those hydrogarnet defects in Si-deficient

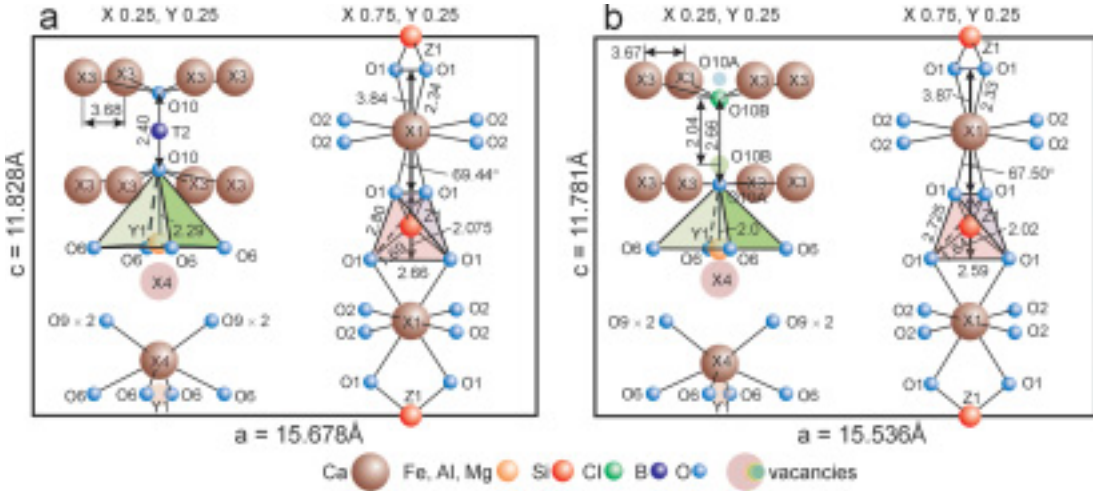

FIG. 3. Portions of the structure of *P*/4*nnc* vesuvianite showing the string-like arrangement of atoms along the **c** axis. a. Silicon-deficient boron-bearing vesuvianite; b. fluorine-bearing chlorine–boron-bearing vesuvianite from Polar Yakutia (Galuskin *et al*. 2003b). Interatomic distances are given in Å; for discussion, see text.

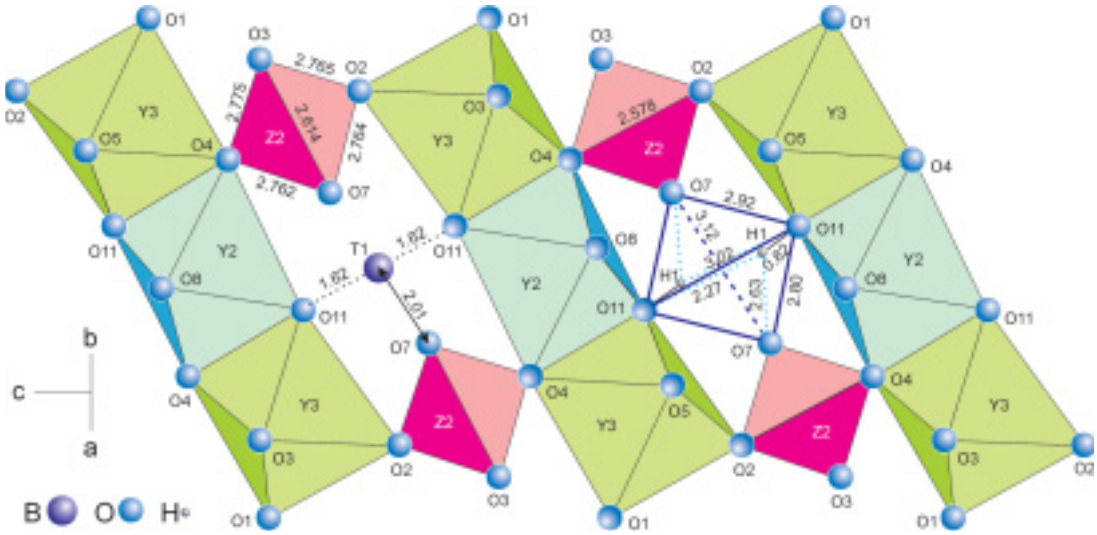

FIG. 4. Fragment of the Si-deficient vesuvianite structure formed by trimers of *Y*(3)–*Y*(2)–*Y*(3) octahedra showing *Z*(2) tetrahedra and the interstitial *T*(1) site. The *T*(1) site is to a very limited degree (*ca*. 7%) occupied by boron, it but generally contains a network of bifurcated hydrogen bonds. Interatomic distances are given in Å.

vesuvianite is not defined. However, an analogous situation occurs in hibschite (Lager *et al*. 1989). If one proton is bonded to *O*(7), a cooperative effect results: *O*(7) will be both donor and acceptor, simultaneously.

In the Raman spectra of vesuvianite, the characteristic bands of OH taking part in weak hydrogen bonding are above 3300 cm^{-1}. Such OH groups are mainly expected for the *O*(11) site. In the Raman spectrum of Si-deficient vesuvianite, a broad asymmetric band centered near 3600 cm^{-1} extends from 3350 to 3720 cm^{-1}. The spectrum is deconvoluted into three lines at 3647.5, 3588 and 3488 cm^{-1} (Fig. 2). For normal (18 Si *pfu*) vesuvianite, polarization (ZZ and ZX) of Raman spectra for the lines near 3670 cm^{-1} (configuration $Mg^{Y(3)}$–$Al^{Y(2)}$–$OH^{O(11)}$) and near 3630 cm^{-1} (configuration $Al^{Y(3)}$–$Al^{Y(2)}$–$OH^{O(11)}$) yields an ZZ/ZX intensity ratio of ~80/20 (Galuskin *et al*. 2007), similar to the polarization behavior of FTIR spectra at corresponding wavelengths (Groat *et al*. 1995, Bellatreccia *et al*. 2005b). For Raman spectra of Si-deficient vesuvianite, this ratio is ~60/40. This more isotropic behavior is attributed to the additional modes of OH groups taking part in hydrogarnet defects. In the Raman spectra of hibschite, the main line characteristic of OH-stretching vibrations is near 3650 cm^{-1} (Kolesov & Geiger 2005). The line at 3647.5 cm^{-1}, obtained by spectral decomposition of spectra of the Si-deficient vesuvianite, is probably associated with the hydrogarnet defects.

Acknowledgements

We thank L.A. Groat, G. Della Ventura, and R.F. Martin for their constructive comments on this paper. Financial support for this project was provided partly by the Scientific Research fund of the KBN (Polish Committee of Research) grant 3P04D 03622.

References

Allen, F.M. & Burnham, C.W. (1992): A comprehensive structure-model for vesuvianite: symmetry variations and crystal growth. *Can. Mineral*. **30**, 1-18.

Armbruster, T. & Gnos, E. (2000a): *P*4/*n* and *P*4*nc* long-range ordering in low-temperature vesuvianites. *Am. Mineral*. **85**, 563-569.

Armbruster, T. & Gnos, E. (2000b): Tetrahedral vacancies and cation ordering in low-temperature Mn-bearing vesuvianites: indication of hydrogarnet-like substitution. *Am. Mineral*. **85**, 570-577.

Armbruster, T. & Gnos, E. (2000c): "Rod" polytypism in vesuvianite: crystal structure of a low-temperature *P*4*nc* with pronounced octahedral cation ordering. *Schweiz. Mineral. Petrogr. Mitt*. **80**, 109-116.

Armbruster, T., Gnos, E., Dixon, R., Gutzmer, J., Hejny, C., Döbelin, N. & Medenbach, O. (2002): Manganvesuvianite and tweddillite, two new Mn^{3+}-silicate minerals from the Kalahari manganese fields, South Africa. *Mineral. Mag*. **66**, 137-150.

Bellatreccia, F., Cámara, F., Ottolini, L., Della Ventura, G., Cibin, G. & Mottana, A. (2005a): Wiluite from Ariccia, Latium, Italy: occurrence and crystal structure. *Can. Mineral*. **43**, 1457-1468.

Bellatreccia, F., Della Ventura, G., Ottolini, L., Libowitzky, E. & Beran, A. (2005b): The quantitative analysis of OH in vesuvianite: a polarized FTIR and SIMS study. *Phys. Chem. Minerals* **32**, 65-76.

Britvin, S.N., Antonov, A.A., Krivovichev, S.V., Armbruster, T., Burns, P.C. & Chukanov, N.V. (2003): Fluorvesuvianite, $Ca_{19}(Al,Mg,Fe^{2+})_{13}[SiO_4]_{10}[Si_2O_7]_4O(F,OH)_9$, a new mineral species from Pitkäranta, Karelia, Russia: description and crystal structure. *Can. Mineral*. **41**, 1371-1380.

Coda, A., Della Giusta, A., Isetti, G. & Mazzi, F. (1970): On the crystal structure of vesuvianite. *Atti Accad. Sci. Torino* **105**, 63-84.

Fitzgerald, S., Leavens, P.B. & Nelen, J.A. (1992): Chemical variation in vesuvianite. *Mineral. Petrol*. **46**, 163-178.

Fitzgerald, S., Rheingold, A.L. & Leavens, P.B. (1986): Crystal structure of non-*P*4/*nnc* vesuvianite from Asbestos, Quebec. *Am. Mineral*. **71**, 1483-1488.

Galuskin, E.V. (2005): *Minerals of Vesuvianite Group from Achtarandite Rocks (Wiluy River, Yakutia)*. University of Silesia, Katowice, Poland (in Polish).

Galuskin, E.V., Armbruster, T., Malsy, A., Galuskina, I.O. & Sitarz, M. (2003b): Morphology, composition and structure of low-temperature *P*4/*nnc* high-fluorine vesuvianite whiskers from Polar Yakutia, Russia. *Can. Mineral*. **41**, 843-856.

Galuskin, E.V., Galuskina, I.O. & Dzierżanowski, P. (2005): Chlorine in vesuvianites. *Mineral. Polon*. **36**(1), 51-61.

Galuskin, E.V. & Galuskina, I.O. (2002): Achtarandite – sponge hibschite pseudomorph after wadalite-like phase: internal morphology and mechanism of formation. *Neues Jahrb. Mineral., Abh*. **178**, 63-74.

Galuskin, E.V., Galuskina, I.O., Sitarz, M. & Stadnicka, K. (2003a): Si-deficient, OH-substituted, boron-bearing vesuvianite from the Wiluy River, Yakutia, Russia. *Can. Mineral*. **41**, 833-842.

Galuskin, E.V., Galuskina, I.O. & Winiarska, A. (1995): Epitaxy of achtarandite on grossular – the key to the problem of achtarandite. *Neues Jahrb. Mineral., Monatsh*., 306-320.

Galuskin, E.V., Janeczek, J., Kozanecki, M., Sitarz, M., Jastrzębski, W., Wrzalik, R. & Stadnicka, K. (2007): Single-crystal Raman investigation of vesuvi-

anite in the OH region. *Vib. Spectrosc.*, doi:10.1016/j.vibspec.2006.06.22.

GALUSKINA, I.O., GALUSKIN, E.V. & SITARZ, M. (1998): Atoll hydrogarnets and mechanism of the formation of achtarandite pseudomorphs. *Neues Jahrb. Mineral., Monatsh.*, 49-62.

GROAT, L., HAWTHORNE, F.C. & ERCIT, T.S. (1992): The chemistry of vesuvianite. *Can. Mineral.* **30**, 19-48.

GROAT, L., HAWTHORNE, F.C. & ERCIT, T.S. (1994): The incorporation of boron into the vesuvianite. *Can. Mineral.* **32**, 505-523.

GROAT, L., HAWTHORNE, F.C., ERCIT, T.S. & GRICE, J.D. (1998): Wiluite $Ca_{19}(Al,Mg,Fe,Ti)_{13}(B,Al,\square)_5Si_{18}O_{68}(O,OH)_{10}$, a new mineral species isostructural with vesuvianite, from the Sakha Republic, Russian Federation. *Can. Mineral.* **36**, 1301-1304.

GROAT, L., HAWTHORNE, F.C., LAGER, G.A., SCHULTZ, A.J. & ERCIT, T.S. (1996): X-ray and neutron crystal-structure refinements of boron-bearing vesuvianite. *Can. Mineral.* **34**, 1059-1070.

GROAT, L., HAWTHORNE, F.C., ROSSMAN, G.R. & ERCIT, T.S. (1995): The infrared spectroscopy of vesuvianite in the OH region. *Can. Mineral.* **33**, 609-626.

HENMI, C., KUSACHI, I. & HEMNI, K. (1994): Vesuvianite from Kushiro, Hiroshima Prefecture, Japan. *Int. Mineral. Assoc., 16th Gen. Meeting* (*Pisa*), *Program Abstr.*, 172-173.

KOLESOV, B.A. & GEIGER, C.A. (2005): The vibrational spectrum of synthetic hydrogrossular (katoite) $Ca_3Al_2(O_4H_4)_3$: a low-temperature IR and Raman spectroscopic study. *Am. Mineral.* **90**, 1335-1341.

LAGER, G.A., ARMBRUSTER, T., ROTELLA F.J. & ROSSMAN, G.R. (1989): OH substitution in garnets: X-ray and neutron diffraction, infrared, and geometric-modelling studies. *Am. Mineral.* **74**, 840-851.

LAGER, G.A., XIE, Q., ROSS, F.K., ROSSMAN, G.R., ARMBRUSTER, T., ROTELLA, F.J. & SCHULTZ, A.J. (1999): Hydrogen-atom position in *P*4/*nnc* vesuvianite. *Can. Mineral.* **37**, 763-768.

LIBOWITZKY, E. (1999): Correlation of O–H stretching frequencies and O–H...O hydrogen bond lengths in minerals. *Monatsh. Chem.* **130**, 1047-1059.

LYAKHOVICH, V.V. (1954): New data for mineralogy of Wiluy deposit of achtarandite. *Trudy Vostochno-sibirskogo filiala Akad. Nauk SSSR, Seria Geol.* **1**, 85-116 (in Russ.).

OHKAWA, M. (1994): Crystal chemistry and structure of vesuvianite. *J. Sci. Hiroshima Univ., Ser.* **C**, **10**, 119-149.

PALUSZKIEWICZ, C. & ŻABIŃSKI, W. (1995): H-bonding in vesuvianites, a complex ortho-disilicate. *Vibr. Spectrosc.* **8**, 315-318.

PALUSZKIEWICZ, C. & ŻABIŃSKI, W. (1999): NIR spectra of vesuvianite – a complex ortho-disilicate mineral. *J. Mol. Struct.* **480–481**, 683-688.

PALUSZKIEWICZ, C. & ŻABIŃSKI, W. (2004): Vibrational spectroscopy as a tool for discrimination of high and low vesuvianites. *Vibr. Spectrosc.* **35**, 77-80.

PAVESE, A., PRENCIPE, M., TRIBAUDINO, M. & AAGAARD, S.S. (1998): X-ray and neutron single-crystal study of *P*4/*n* vesuvianite. *Can. Mineral.* **36**, 1029-1037.

SHELDRICK, G.M. (1997): *SHELX–97, Program for Crystal Structure Determination*. University of Göttingen, Göttingen, Germany.

TRIBAUDINO, M. & PRENCIPE, M. (2001): The compressional behavior of *P*4/*n* vesuvianite. *Can. Mineral.* **39**, 145-151.

WARREN, B.E. & MODELL, D.I. (1931): The structure of vesuvianite $Ca_{10}Al_4(Mg,Fe)_2Si_9O_{34}(OH)_4$. *Z. Kristallogr.* **78**, 422-432.

YOSHIASA , A. & MATSUMOTO, T. (1986): The crystal structure of vesuvianite from Nakatasu mine: reinvestigation of the cation site-populations and of the hydroxyl groups. *Mineral. J.* **13**, 1-12.

Received December 27, 2005, revised manuscript accepted June 26, 2006.